

Quantum Criticality in YbRh_2Si_2

Philipp Gegenwart, Jeroen Custers, Stefan Mederle, Karl Neumaier*, Julia Ferstl, Günter Sparn, Christoph Geibel, Heribert Wilhelm and Frank Steglich

One of the main research activities at the Institute in the past years was the study of quantum criticality in heavy fermion (HF) systems. Quantum phase transitions, in contrast to their classical counterparts at $T > 0$ where thermal fluctuations are important, are driven by a control parameter other than temperature, e.g., chemical composition or pressure. A quantum critical point (QCP) commonly separates an ordered from a disordered phase at $T = 0$. The understanding of Non-Fermi liquid (NFL) effects that occur close to the antiferromagnetic (AF) QCP in HF systems is one of the major and most controversially discussed problems in condensed matter physics.

Two different scenarios for the QCP, where long-range AF order emerges from the HF state, have been proposed: a *spin density wave* (SDW) and a *localized moment* (LM) scenario. In the former scenario [1,2], magnetic properties are associated with the spin polarization of the Fermi surface and NFL behavior results from the scattering of quasiparticles (QP) off the quantum-critical spin fluctuations in the magnetization. Three dimensional (3D) spin fluctuations only couple strongly to QP along *hot lines* around the Fermi surface separated by the wave vector \mathbf{Q} of the AF order. The remaining part of the Fermi surface is largely unaffected by the quantum critical fluctuations. Only in the case of strong magnetic frustration the 3D system of AF spin fluctuations (“spin fluid”) may be decoupled into 2D spin fluids that render the entire Fermi surface “hot” (2D SDW scenario) [3]. Very recent inelastic neutron scattering experiments on $\text{CeCu}_{5.9}\text{Au}_{0.1}$ revealed an anomalous energy over temperature, E/T , scaling in the critical component of the AF spin fluctuations that is almost momentum independent, i.e. local in nature [4]. This has led to the proposal that the LM scenario [5,6] in which the internal structure of the composite fermions is seriously taken into account, is more adequate for HF metals than the (itinerant) SDW scenario.

The tetragonal compound YbRh_2Si_2 [7] is ideally suited to study quantum critical effects because (i) it is located remarkably close to an AF QCP with a

tiny ordering temperature of $T_N = 70$ mK (Fig. 1a) and (ii) the effect of disorder is negligible in clean single crystals with residual resistivities as low as $1 \mu\Omega\text{cm}$ (Fig. 1d) [8]. The application of pressure to YbRh_2Si_2 [9] increases T_N as expected, because the ionic volume of the magnetic ($4f^{13}$) Yb^{3+} -configuration is smaller than that of the nonmagnetic ($4f^{14}$) Yb^{2+} one. Expanding the crystal lattice by randomly substituting Ge for the smaller isoelectric Si atoms allows one to tune $\text{YbRh}_2(\text{Si}_{1-x}\text{Ge}_x)_2$ towards the QCP without affecting its electronic properties and without introducing significant disorder to the lattice [10]. A nominal Ge concentration $x = 0.05$ (a microprobe analysis revealed an actual concentration $x \leq 0.02$) was recently shown to push T_N down to 20 mK (Fig. 1a). The comparison of the T_N vs pressure phase diagrams of the undoped and the $x = 0.05$ single crystal (Fig. 1c) proves that the main effect of Ge doping is indeed the expansion of the lattice. The pressure shift of -0.2 GPa [10] corresponds to a volume expansion

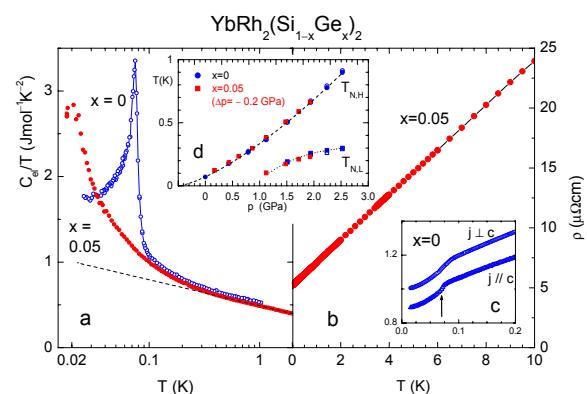


Fig. 1: Electronic specific heat coefficient (a) and electrical resistivity (b and c) of $\text{YbRh}_2(\text{Si}_{1-x}\text{Ge}_x)_2$ single crystals with Ge-contents $x = 0$ (blue symbols) and nominal $x = 0.05$ (red symbols). (d): Pressure dependence of AF phase transition temperatures in $\text{YbRh}_2(\text{Si}_{1-x}\text{Ge}_x)_2$ as deduced from electrical resistivity measurements for $x = 0$ and $x = 0.05$. Data for the latter sample are shifted uniformly by $\Delta p = -0.2$ GPa. Dotted line in (a) marks $\log(T_0/T)$ with $T_0 = 24$ K. The arrow in (c) indicates T_N .

of 0.1% for the Ge-doped sample, consistent with a true Ge content of 0.02 ± 0.004 .

In undoped YbRh_2Si_2 the resistivity follows a quasi-linear T -dependence down to about 80 mK, below which a sharp decrease (independent of the current direction) is observed (Fig. 1d): The resistivity does not show any signatures of a SDW formation for which an increase of $\rho(T)$ along the direction of the SDW modulation, indicating the partial gapping of the Fermi surface, should be expected slightly below T_N . The absence of this behavior favors the interpretation of local-moment type of magnetic order in YbRh_2Si_2 . The resistivity in the AF ordered state ($B = 0$) is best described by $\Delta\rho = \rho - \rho_0 = AT^2$ (ρ_0 : residual resistivity) with a huge coefficient, $A = 22 \mu\Omega\text{cm}/\text{K}^2$ for $20 \text{ mK} \leq T \leq 60 \text{ mK}$ [8]. Extrapolating $\Delta C(T)/T$ as $T \rightarrow 0$ to $\gamma_0 = 1.7 \text{ J}/\text{K}^2\text{mol}$ reveals an entropy gain at the AF phase transition of only about $0.03 \text{ Rln}2$. This is in accordance with the very small value of about $2 \times 10^{-3} \mu_B$ for the ordered moment found in μSR experiments [11] and provides evidence for the weakness of the AF order in YbRh_2Si_2 . The ratio of A/γ_0^2 in the ordered state is close to that expected for a Landau Fermi liquid (LFL) [12], i.e., one with very heavy quasiparticle masses. Both YbRh_2Si_2 and $\text{YbRh}_2(\text{Si}_{1-x}\text{Ge}_x)_2$, $x = 0.05$ (nominal) show very similar behavior at $B = 0$ in their corresponding paramagnetic states. For $0.3 \text{ K} \leq T \leq 10 \text{ K}$, the specific heat coefficient and the electrical resistivity follow $C_{el}(T)/T \propto \log(T_0/T)$ with $T_0 \dagger 24 \text{ K}$

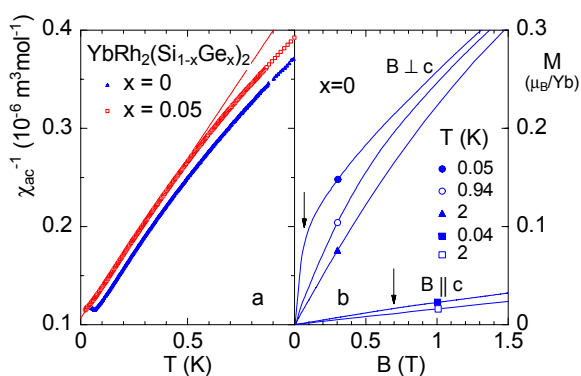


Fig. 2: AC susceptibility of $\text{YbRh}_2(\text{Si}_{1-x}\text{Ge}_x)_2$ measured along the basal plane as χ^{-1} vs T (a). Isothermal DC magnetization at varying temperatures for fields applied along and perpendicular to the c -axis, respectively. The arrows mark the critical fields $B_{c0} = 0.06 \text{ T}$ and 0.7 T for $B \perp c$ and $B \parallel c$, respectively.

have been proposed to describe the asymptotic ($T \rightarrow 0$) behavior in the 2D SDW scenario. Whereas the resistivity continues to follow this linear T -dependence down to below 20 mK, a pronounced upturn occurs in C_{el}/T below 0.3 K whose origin will be discussed at the end. In the same T -range the uniform magnetic susceptibility is well described by a Curie-Weiss law (Fig. 2a) implying a surprisingly large effective moment $\mu_{\text{eff}} \dagger 1.4 \mu_B$ and a Weiss temperature $\Theta \dagger -0.32 \text{ K}$ [8]. Remarkably, this paramagnetic moment exceeds the small ordered moment by more than two orders of magnitude and is observed at temperatures two orders of magnitude smaller than the Kondo temperature scale $T_K = 30 \text{ K}$.

Since T -dependent measurements at the QCP alone provide no information on how the heavy QPs decay into the quantum critical state it is necessary to tune the system away from the magnetic instability into the Landau Fermi liquid (LFL) state and to follow the QP properties upon approaching the QCP. We recently used the application of magnetic fields for this purpose [8]. We first discuss the low-temperature magnetization which proves that the AF phase transition as a function of field is a continuous one. YbRh_2Si_2 exhibits a highly anisotropic magnetic response indicating that Yb^{3+} moments are forming an “easy-plane” square lattice perpendicular to the crystallographic c -direction [7]. The isothermal magnetization (Fig. 2b) shows a strongly nonlinear response for fields

For $T < T_N$ a clear reduction in slope is observed above 0.06 T which indicates the suppression of AF order resulting in a weakly polarized state. For continuous polarization of the paramagnetic moments for fields exceeding the critical field $B_{c0}(0) = 0.06 \text{ T}$ gives rise to a strong curvature in $M(B)$. For $B \geq 10 \text{ T}$ the Kondo interaction appears to be completely suppressed and the moments are not fully aligned. The extremely low value of the critical field for AF order highlights the near proximity of two different heavy LFL states, one being weakly antiferromagnetically ordered ($B < B_{c0}$) and the other being weakly polarized ($B > B_{c0}$). For fields applied along the magnetic hard direction $B \parallel c$, the magnetization shows an almost linear behavior which was found to extend at least up to 10 T [13]. At $T < T_N$ a very tiny increase in the $M(B)$ slope is observed below about 0.7 T which, according to the resistivity measurements discussed below, represents the critical field for $B \parallel c$.

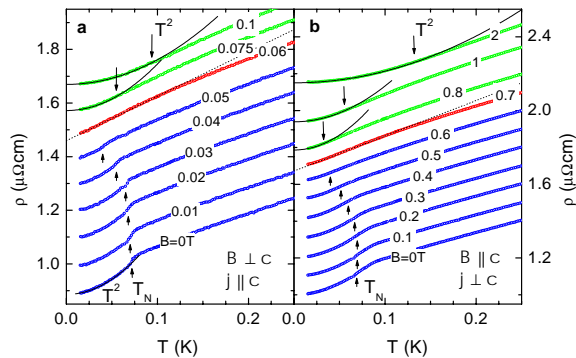


Fig. 3: Low-temperature electrical resistivity of YbRh_2Si_2 at varying magnetic fields applied perpendicular (a) and along the c -axis (b). For clarity the different curves in $B > 0$ were shifted subsequently by $0.1 \mu\Omega\text{cm}$. Up- and down raising arrows indicate T_N and upper limit of T^2 behavior, respectively. Dotted and solid lines represent $\Delta\rho \propto T^\varepsilon$ with $\varepsilon = 1$ and $\varepsilon = 2$, respectively.

In Fig. 3 we show the evolution of the low-temperature resistivity upon applying magnetic fields along and perpendicular to the easy magnetic plane. At small magnetic fields the Néel temperature, determined from the maximum value of $d\rho/dT$, shifts to lower temperatures and vanishes at a critical magnetic field B_{c0} of 0.06 T, applied in the easy magnetic plane, and of 0.66 T, applied along the c -axis. At $B = B_{c0}$, the resistivity follows a linear T -dependence down to the lowest accessible temperature of about 20 mK (red symbols in Fig. 3). This observation provides striking evidence for field-induced NFL behavior at the critical magnetic field applied along either crystallographic direction [8]. At $B > B_{c0}$ we find LFL behavior $\Delta\rho = AT^2$ for $T \leq T^*(B)$ with the characteristic temperature $T^*(B)$ increasing and $A(B)$ decreasing upon raising the applied magnetic field. The evolution of T_N and T^* as a function of B is shown in Fig. 4. As illustrated in Fig. 5, NFL behavior dominates over a wide region of the T - B phase diagram above T_N and $T^*(B)$ including the narrow border regime down to lowest accessible temperature of 20 mK between the two LFL states at $B = B_{c0}$. A very similar observation is made for the $x = 0.05$ sample whose B_{c0} value is shifted very close to zero.

We also investigated the electronic contribution to the low-temperature specific heat at magnetic fields applied along the c -axis. At the critical value B_{c0} a strong divergence is found in C_{el}/T vs. T [8]. At higher fields $B > B_{c0}$, C_{el}/T becomes almost tem-

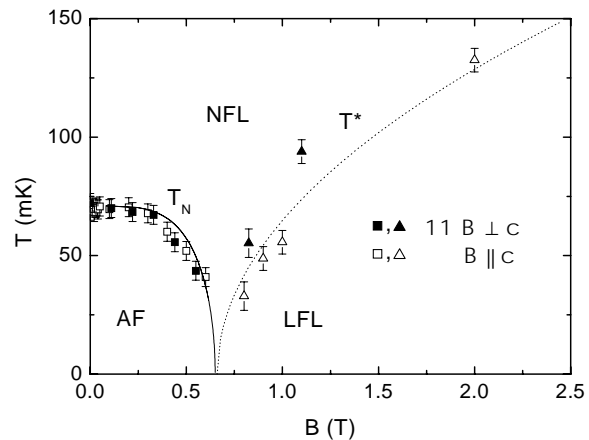


Fig. 4: T - B phase diagram for YbRh_2Si_2 with T_N as derived from $d\rho/dT$ vs T and T^* , the upper limit of the $\Delta\rho = AT^2$ behavior, as a function of magnetic field, applied both parallel and perpendicular to the c -axis. For the latter ones the B -values have been multiplied by a factor 11. Lines separating the antiferromagnetic (AF), non-Fermi liquid (NFL) and Landau Fermi liquid (LFL) phase are guides to the eye.

perature independent at low temperatures, as expected for a LFL, with a strongly field-dependent coefficient $\gamma_0(B)$. Furthermore, a weak maximum is observed at a characteristic temperature $T_0(B)$ which grows linearly with the field indicating that, upon the application of a field, entropy is transferred from the low-temperature upturn to higher temperatures.

In Fig. 6 we present our analysis of the magnetic-field dependence of the coefficients A , γ_0 and χ_0 observed for $T \rightarrow 0$ in the resistivity, $\Delta\rho = A(B)T^2$, specific heat, $C_{el}/T = \gamma_0(B)$, and magnetic AC-susceptibility, $\chi = \chi_0(B)$, when approaching the QCP upon reducing B towards B_{c0} [8]. Since YbRh_2Si_2 behaves as a true LFL for $B > B_{c0}$ and $T < T^*(B)$ the observed temperature dependences should hold down to $T = 0$ and the coefficients γ_0 and A measure the effective quasiparticle (QP) mass and the effective QP-QP scattering cross-section, respectively. $A(B)$ roughly diverges as $(B - B_{c0})^{-1}$ indicating that the whole Fermi surface undergoes singular scattering at the QCP. Within the SDW scenario this would require strictly 2D critical AF spinfluctuations [14]. The same model, however, predicts a logarithmic divergence of $\gamma_0(B)$ for $B \rightarrow B_{c0}$. In contrast, we observe a constant Kadowaki-Woods ratio A/γ_0^2 for $B > 0.5$ T (see inset Fig. 6, [8]) indicating a $B^{-0.5}$ divergence of $\gamma_0(B)$. Very recently, the $\gamma_0(B)$

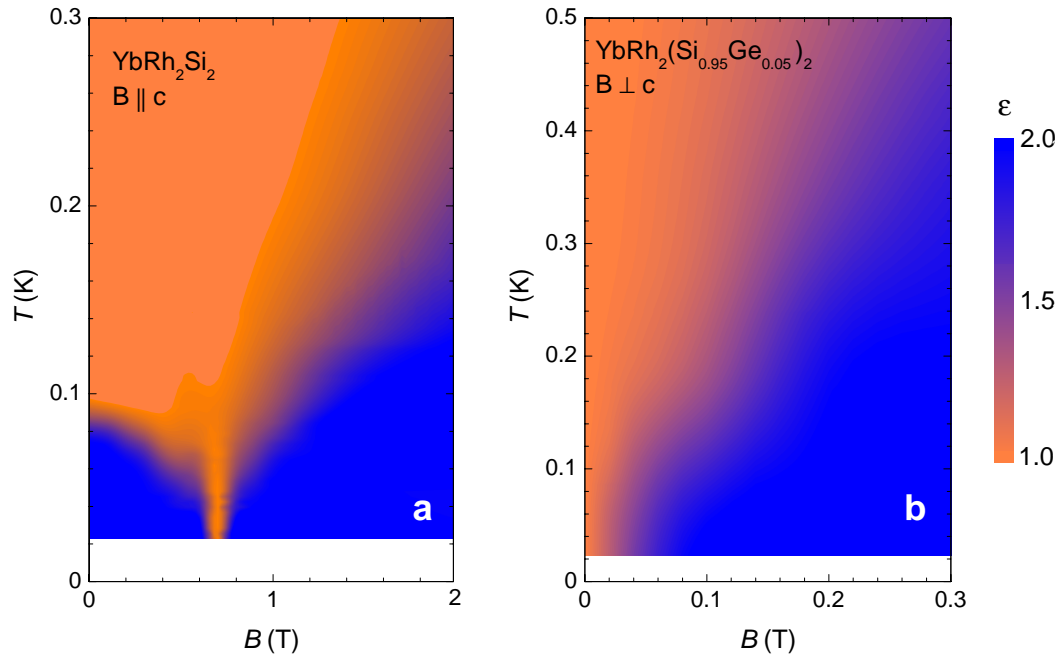


Fig. 5: Color representation of the evolution of the resistivity exponent, ϵ , in the power-law representation $(\rho - \rho_0) \propto T^\epsilon$. Blue (yellow) colors mark Landau Fermi liquid (non-Fermi liquid) behavior characterized by $\epsilon = 2$ ($\epsilon = 1$).

dependence at the field-induced QCP has been studied by careful measurements of the low- T heat capacity of a single crystal of nominal Ge concentration $x = 0.05$, with the magnetic field applied within the easy plane [15]. For this configuration, the critical field is 0.027 T only. Most importantly,

a power law divergence $\gamma_0(B) \sim (B - B_c)^{-0.33}$ is observed upon reducing $(B - B_c)$ from 1 T down to 0.02 T [15]. This provides clear evidence for a stronger-than-logarithmic mass divergence at the QCP *incompatible with the SDW scenario*. Furthermore, the observed field dependence in $\gamma_0(B)$ proves that the zero-field ‘‘upturn’’ in $C_{el}(T)/T$ below 0.3 K for $\text{YbRh}_2(\text{Si}_{0.95}\text{Ge}_{0.05})_2$ (Fig. 1a) is intrinsic and related to the QCP. The Curie-Weiss behavior, observed in $\chi(T)$ in the same T -range (Fig. 2a), hints to large unscreened fluctuating Yb^{3+} moments persisting all the way down to the QCP. This strongly suggests a local nature of the critical fluctuations.

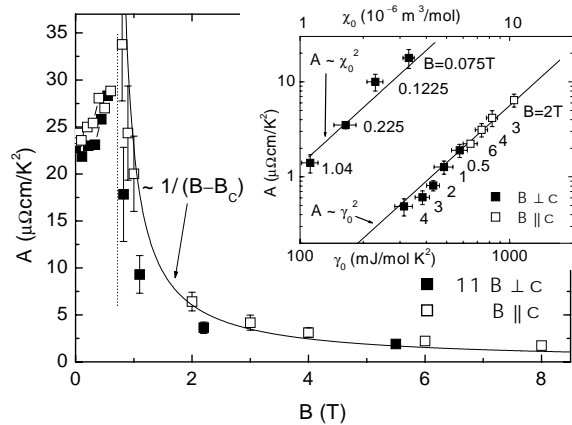


Fig. 6: Coefficient $A = \Delta\rho/T^2$ vs field B . Data for B perpendicular to the c -direction have been multiplied by 11. Dashed line marks B_{c0} , solid line represents $(B - B_{c0})^{-1}$. Inset shows double-log plot of A vs. γ_0 and A vs. χ_0 for different magnetic fields. Solid lines represent $A/\gamma_0^2 = 5.8 \times 10^{-6} \mu\Omega\text{cm}(\text{Kmol/mJ})^2$ and $A/\chi_0^2 = 1.25 \times 10^{12} \mu\Omega\text{cm K}^{-2}/(\text{m}^3/\text{mol})^2$.

The electrical resistivity in the paramagnetic state does not show any cross-over but strictly follows a linear T -dependence from $T \leq 10$ K down to the lowest temperatures (Fig. 1b). This striking disparity at low T between the thermodynamic quantity $\gamma_0(T) = C_{el}(T)/T$ and the transport property $\Delta\rho(T)$ suggests that the dominating local f -component of the composite fermions, probed by $\gamma_0(T)$, is more sensitive to the nearby AF order than its itinerant counterpart probed by $\Delta\rho(T)$. The observed disparity may thus be viewed as a direct manifestation of a real *break up of the composite fermion* in the approach to the QCP [15].

References

- [1] *J. A. Hertz*, Phys. Rev. B **14**, 1165 (1976).
- [2] *A. J. Millis*, Phys. Rev. B **48**, 7183 (1993).
- [3] *A. Rosch, A. Schröder, O. Stockert, and H. v. Löhneysen*, Phys. Rev. Lett. **79**, 159 (1997).
- [4] *A. Schroeder, G. Aeppli, R. Coldea, M. Adams, O. Stockert, H. v. Löhneysen, E. Bucher, R. Ramazashvili, and P. Coleman*, Nature **407**, 351 (2000).
- [5] *Q. Si, S. Rabello, K. Ingersent, and J. L. Smith*, Nature **413**, 804 (2001).
- [6] *P. Coleman and C. Pépin*, Physica B **312**, 383-389 (2002).
- [7] *O. Trovarelli, C. Geibel, S. Mederle, C. Langhammer, F. M. Grosche, P. Gegenwart, M. Lang, G. Sparn, and F. Steglich*, Phys. Rev. Lett. **85**, 626 (2000).
- [8] *P. Gegenwart, J. Custers, C. Geibel, K. Neumaier, T. Tayama, K. Tenya, O. Trovarelli, and F. Steglich*, Phys. Rev. Lett. **89**, 056402 (2002).
- [9] *S. Mederle, R. Borth, C. Geibel, F.M. Grosche, G. Sparn, O. Trovarelli, and F. Steglich*, J. Phys: Condens. Matt. **14** (2002) 10731.
- [10] *O. Trovarelli, J. Custers, P. Gegenwart, C. Geibel, P. Hinze, S. Mederle, G. Sparn, and F. Steglich*, Physica B **312-313**, 401 (2002).
- [11] *K. Ishida, D. E. MacLaughlin, Ben-Li Young, K. Okamoto, Y. Kawasaki, Y. Kitaoka, G. J. Nieuwenhuys, R. H. Heffner, O. O. Bernal, W. Higemoto, A. Koda, R. Kadono, O. Trovarelli, C. Geibel, and F. Steglich*, to be published.
- [12] *K. Kadowaki and S.B. Woods*, Sol. State Commun. **58**, 507 (1986).
- [13] *J. Custers, P. Gegenwart, C. Geibel, F. Steglich, T. Tayama, O. Trovarelli, and N. Harrison*, Acta Phys. Pol. **B32**, 3221 (2001).
- [14] *I. Paul and G. Kotliar*, Phys. Rev. B **64**, 184414 (2001).
- [15] *J. Custers, P. Gegenwart, H. Wilhelm, K. Neumaier, Y. Tokiwa, O. Trovarelli, C. Geibel, F. Steglich, C. Pépin, and P. Coleman*, to be published.

* Walther Meissner Institute for Low Temperature Research of the Bavarian Academy of Sciences 85748 Garching, Germany